Electronic structure at highly ordered organic/metal interfaces: Pentacene on Cu(110)

H. Yamane,[1] D. Yoshimura,[2] E. Kawabe,[1] R. Sumii,[3] K. Kanai,[3] Y. Ouchi,[1] N. Ueno,[4,5] and K. Seki[1,3,6]
[1]*Department of Chemistry, Graduate School of Science, Nagoya University, Nagoya 464-8602, Japan*
[2]*SAGA Light Source, Kyushu Synchrotron Light Research Center, Saga 841-0005, Japan*
[3]*Research Center for Materials Science, Nagoya University, Nagoya 464-8602, Japan*
[4]*Graduate School of Advanced Integration Science, Chiba University, Yayoi-cho, Inage-ku, Chiba 263-8522, Japan*
[5]*Center for Frontier Science, Chiba University, Yayoi-cho, Inage-ku, Chiba 263-8522, Japan*
[6]*Institute for Advanced Research, Nagoya University, Nagoya 464-8602, Japan*
(Received 24 April 2007; revised manuscript received 23 July 2007; published 29 October 2007)

The electronic structure at highly ordered pentacene monolayer prepared on Cu(110) substrate was studied by angle-resolved ultraviolet photoemission spectroscopy. The valence-level photoemission line shape showed the evidences of (i) formation of the interface states and (ii) two-dimensional energy-band dispersion of the resultant interface states. The lattice constant deduced from the observed energy-band dispersion is consistent with the reported one based on the low-energy electron diffraction experiments. Thus, the observed energy-band dispersion can be ascribed to the in-plane intermolecular energy-band dispersion in the pentacene monolayer on Cu(110). These phenomena may originate from the hybridization between the molecular orbital and the wave function of the substrate surface. Furthermore, work-function change of about −0.9 eV by adsorption of pentacene was observed from the shift of the secondary-electron cutoff. Such a decrease of the work function indicates the formation of a dipole layer at the interface with the molecule positively charged. This direction is opposite to the naive expectation from the electron transfer from the substrate to the molecule, which was suggested from the previous work of core-level photoemission spectroscopy [McDonald *et al.*, Surf. Sci. **600**, 1909 (2006)]. This unexpected result may originate from the charge redistribution at the interface due to the induced image charge in the metal and the push back of electrons spilled out from the metal surface by the adsorbed molecules, which may overwhelm the effect of electron transfer.

DOI: 10.1103/PhysRevB.76.165436 PACS number(s): 79.60.−i, 73.20.−r, 73.30.+y, 72.80.Le

I. INTRODUCTION

The electronic structure at interfaces formed between an organic film and a metal surface plays a crucial role in the performance of (opto)electronic devices using organic semiconductors such as light-emitting diodes, field-effect transistors, and photovoltaic cells. In particular, the energy positions of the highest-occupied and lowest-unoccupied molecular orbital (HOMO and LUMO) levels relative to the Fermi level (E_F) of metal electrodes are of fundamental importance in discussing the barrier heights for the charge injection and separation at organic/metal interfaces.[1,2] Therefore, it is natural that many research groups have been investigating the energy level alignment at organic-related interfaces in order to elucidate the energetics of organic devices.[1–20] These studies have been performed by using surface-scientific tools such as ultraviolet photoemission spectroscopy (UPS), inverse photoemission spectroscopy, Kelvin probe, scanning tunneling microscopy (STM), and scanning tunneling spectroscopy (STS), which provide the information on the occupied and unoccupied electronic structures and the vacuum level.

By these studies, it is now well established that the formation of the interfacial electric dipole layer affects the energy level alignment and, hence, the barrier heights at the interface.[1,2] Thus, the clarification of the origin of this interface dipole is an important issue in the recent studies of organic interfaces. Several possible factors were listed as possible origins,[1] and there are already evidences for (1) electron transfer between the molecule and the metal for strong donors and acceptors,[8,9] and (2) the orientation of polar molecules[10–13] as the origin of the dipole layer. On the other hand, the origin and the details of the dipole layer for ordinary nonpolar molecules with moderate electron donating and/or accepting power have not yet been well clarified. Among the efforts for clarifying the responsible factors, Flores and co-workers recently proposed the concepts of the induced density of interface states[21] (IDIS) and the charge neutrality level (CNL) to describe the dipole layer formation in terms of the molecular level broadening by the molecule-metal interaction.[22–24] Their basic idea is as follows. The HOMO and LUMO are simply broadened to form a continuous density of states (IDIS) in the original HOMO-LUMO gap of the molecule, and the two electrons in the original HOMO occupy these states up to the CNL. At electrical equilibrium after the contact, the initial energy difference between the E_F of the metal and the CNL of the organic semiconductor is cancelled to achieve thermodynamic and electrical equilibria with the alignment of the top occupied states at both sides of the interface by (1) some amount of electron transfer and (2) the accompanying change of the electric potential including the effect of the dielectric constant of the organic layer. This process determines the amount and direction of charge transfer, and the resultant dipole layer is given by the potential change, which corresponds to the work-function change at the deposition of molecules.

They further argued that such broadening of the HOMO and LUMO does not depend on the metal nor the type of surface [(100), (111), etc.], and the energy of the CNL relative to the HOMO and LUMO is a parameter specific to each

molecular species. Their estimation of the dipole layer based on this model showed fair agreement with experiments for various organic films on polycrystalline metal substrates, and they concluded that a simple model holds, with the CNL being actually an intrinsic energy parameter for each organic material, nearly independent of the metal substrate.[22–24]

However, as suggested in our previous work,[1] there are other important possible origins of the interface dipole besides the simple charge transfer. In fact, several groups showed fair agreement between their theoretical calculations and experiments by considering other types of charge redistribution upon molecular adsorption at the surface.[25–27] Thus, the origin of the interface dipole at organic-related interfaces still remains an open question. There are also various observations questioning the picture of simple broadening, mostly independent of the metal surface. Munakata *et al.* observed large spatial inhomogeneity of the electronic structure of Cu-phthalocyanine films on a polycrystalline Cu substrate by using the new techniques of microspot photoemission spectroscopy,[4] and ascribed this inhomogeneity to the difference of molecule-substrate interaction depending on the surface. Several works directly observing the interfacial electronic states by conventional UPS[7] and high-resolution STM with STS[16–20] also indicated that the characteristics of the interfacial electronic structure strongly depend on the substrate surface [e.g., Ag(111) and Ag(110)] and the film structure. Thus, it seems that the factors determining the interfacial electronic structure and the energy level alignment, including the dipole layer, can be more complex than expected in the simple charge-transfer model assuming molecule-specific CNL. Hence, it is generally not easy to discuss the interfacial electronic structure precisely using conventional organic/metal interfaces such as the polycrystalline or amorphous organic films formed on polycrystalline and rough metal surfaces as used in real devices. To fully clarify the possibly complicated electrical and structural phenomena at the organic-related interface, a more pertinent experimental approach to this issue would be to use a well-characterized system, e.g., epitaxially grown organic film on atomically flat and clean metal single crystal surfaces, in quantitative electron spectroscopic measurements.

In this work, in order to study the electronic structure at organic/metal interfaces in detail, we have performed angle-resolved UPS (ARUPS) experiments on a highly ordered pentacene monolayer grown on Cu(110) substrate. It was reported that pentacene molecules on Cu(110) in the monolayer regime form a highly ordered structure with planar adsorption geometry, where the molecular long axis is parallel to the $[1\bar{1}0]$ substrate direction.[28–31] We observed a distinctive electronic structure at the pentacene/Cu(110) interface, which is completely different from those of the gas- and bulk-phase pentacene. We clearly observed the formation of the interface states upon adsorption of the pentacene molecule. Furthermore, the observed interface states shifted periodically with the photoelectron takeoff angle, which can be attributed to the intermolecular energy-band dispersion in the pentacene monolayer. These phenomena may originate from the hybridization between the molecular orbital (MO) and the wave function of the substrate. Also, we discuss the possible origin of the interface dipole at the pentacene/Cu(110) interface.

II. EXPERIMENTS

The experiments were performed using the ARUPS system at the beamline 8B2 of the synchrotron radiation facility UVSOR at the Institute for Molecular Science. The system consists of an organic-preparation chamber, a metal-preparation chamber, and a measurement chamber, with base pressures of 9×10^{-8}, 1×10^{-8}, and 2×10^{-8} Pa, respectively. A Cu(110) single crystal substrate (purity of 5*N*) was purchased from MaTecK GmbH, and was cleaned by repeated cycles of Ar^+ ion sputtering (primary electron-beam energy of 2 keV and current density of about 30 mA/cm^2 under Ar pressure of 8×10^{-3} Pa) and annealing up to about 870 K in the metal-preparation chamber. The cleanliness and the order of atomic arrangements of the substrate surface were confirmed by Auger electron spectroscopy, low-energy electron diffraction (LEED), and UPS measurements.

The purified pentacene sample was the same as that used in Ref. 32. The sample material was purchased from Tokyo Chemical Industry Co., Ltd. (purity 98%), and was purified by three cycles of sublimation in an Ar gas stream of 13 Pa. This material was carefully evaporated onto the clean Cu(110) surfaces in the manner similar to that described in Refs. 30 and 31. In particular, the most important parameter in preparing the highly ordered pentacene monolayer on Cu(110) is the substrate temperature during the deposition. We obtained the highly ordered monolayer by heating the substrate at 500–600 K during the deposition (see Fig. 3 and corresponding discussion). The film thickness and the deposition rate (less than 0.1 nm/min) were measured with a calibrated quartz microbalance.

ARUPS measurements were performed by using a VG-ARUPS10 system with a hemispherical electron energy analyzer and a multichannel detector in the measurement chamber. The synchrotron radiation was monochromatized by a plane-grating monochromator.[33] In the present experiments, we set the total-energy and angular resolutions at about 100 meV and 2°, respectively. The definition of the experimental geometry of ARUPS such as the photon incidence angle (α), photoelectron takeoff angle (θ), and sample azimuthal angle (ϕ) is shown in Fig. 1. The origin of the azimuthal angle $\phi=0°$ was defined so that the electric-field vector ($\boldsymbol{E}$) of the incident photon is on the incident plane containing the $[1\bar{1}0]$ substrate direction and the surface normal (the [110] substrate direction).

All the spectra were measured at the substrate temperature of about 300 K. In order to estimate the work function of the sample, the ARUPS spectra in the region of the secondary-electron cutoff were measured with a −5 V bias applied to the sample to detect the photoelectrons with a kinetic energy (E_k) close to 0 eV.

III. RESULTS AND DISCUSSION

A. Effect of the geometrical film structure on the ultraviolet photoelectron spectroscopy spectra

Prior to showing the experimental results, we briefly summarize the results of the previous works on the growth of

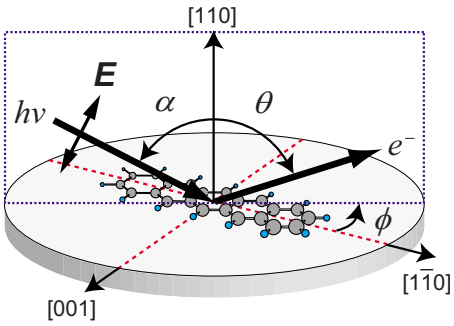

FIG. 1. (Color online) Parameters for experiments of photoelectron angular distribution: the photon incidence angle, electron take-off angle, and sample azimuthal angle are denoted by α, θ, and ϕ, respectively.

pentacene thin films on Cu(110) in the monolayer regime. Highly ordered pentacene monolayer on Cu(110) has been observed and studied by using STM,[28,29] LEED,[29–31] He-atom scattering (HAS),[31] thermal desorption spectroscopy,[31] near-edge x-ray absorption fine structure (NEXAFS),[30,31] and x-ray photoemission spectroscopy (XPS),[15] with mostly consistent results as follows. When the molecules are deposited onto the substrate at room temperature (RT), a disordered pentacene ultrathin film with the molecular long axis parallel to the [1$\bar{1}$0] substrate direction is obtained. After annealing the RT-deposited ultrathin film at 400 K, the molecules (re)order to form a highly ordered (sub-)monolayer with the stripes of pentacene along the [001] substrate direction, retaining the orientation of the molecule with its long axis along the [1$\bar{1}$0] substrate direction.[28] Such a highly ordered monolayer could be also obtained by depositing the molecules on heated substrate at 460 K.[30,31] The LEED patterns of the highly ordered pentacene monolayer on Cu(110) show a predominant $p(6.5\times2)$ [or $p(6\times2)$] structure, while a coexisting $c(13\times2)$ [or $c(12\times2)$] phase was also occasionally observed.[29–31] The surface Brillouin zone for the Cu(110) surface, the $p(6.5\times2)$ overlayer, and the $c(13\times2)$ overlayer are illustrated in Fig. 2.

Figure 3 shows the ARUPS spectra in the regions of the secondary-electron cutoff and the valence levels for the pentacene monolayer on Cu(110); the spectra of the Cu(110) substrate, the 0.3-nm-thick film deposited at 300 K substrate temperature [film (i)], and the monolayer film prepared by depositing the molecules at 500 K substrate temperature [film (ii)] are compared. The abscissa is the binding energy (E_b) relative to the substrate E_F. In order to obtain strong emission just above the vacuum level and the pentacene-derived valence levels, the emission angles of θ=0° and 58° were selected, respectively, with α=60°, ϕ=0°, and the photon energy ($h\nu$)=20 eV.

The spectrum of the clean Cu(110) surface shows an intense peak at 1.9 eV (labeled S), which is attributed to the direct transition from the s,p band of the clean Cu substrate.[34–36] We followed the dispersion with θ of the peak S along the [1$\bar{1}$0] direction, which agrees well with the previous reports.[34–36] For film (i), a pentacene-derived peak appears at 1.0 eV (labeled A), and the work function is decreased by about 0.9 eV from that of the clean substrate (4.6 eV). For film (ii), the peak A becomes more intense, and the work function slightly decreases further from that of the film (i) (0.05 eV). When we annealed film (i) at 600 K, the valence electronic structure and the work function of the an-

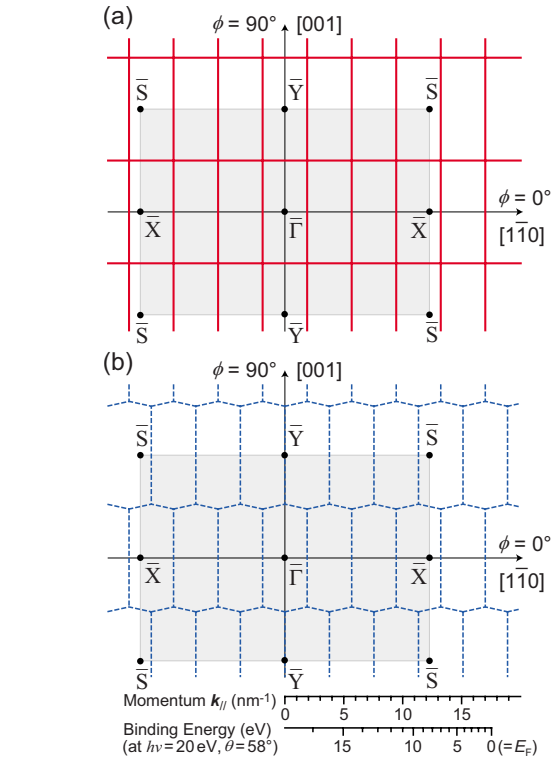

FIG. 2. (Color online) Sketch of the surface Brillouin zone at the pentacene/Cu(110) interface: (a) the $p(6.5\times2)$ overlayer (solid/red line) and (b) $c(13\times2)$ overlayer (dashed/blue line). The first Brillouin zone of the substrate is shown by the gray area.

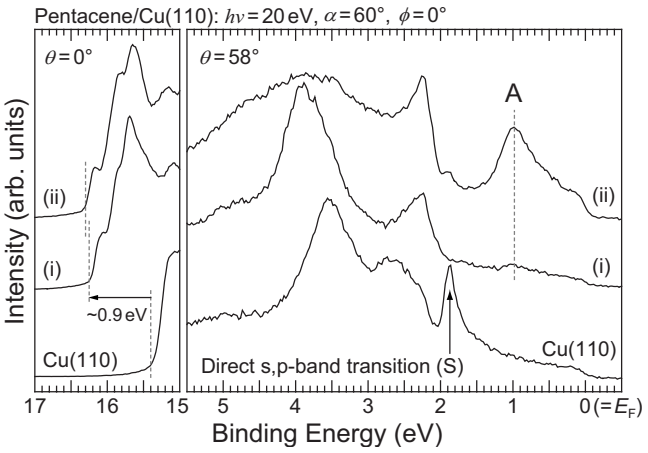

FIG. 3. ARUPS spectra in the regions of the secondary-electron cutoff and the valence levels for the pentacene/Cu(110): the Cu(110) substrate, the 0.3-nm-thick film deposited at 300 K substrate temperature [film (i)], and the monolayer film prepared by depositing the molecules at 500 K substrate temperature [film (ii)]. The abscissa is the binding energy relative to the Fermi level (E_F) of the substrate.

nealed film showed fair agreement with those of film (ii) (not shown). This temperature dependence in the ARUPS spectra corresponds well with the STM observation of the formation of the highly ordered pentacene monolayer at similar annealing reported by Lukas *et al.*, where the molecule orients with its long axis along the $[1\bar{1}0]$ substrate direction.[28] We note that there is a possibility of the presence of the bilayer domain in film (i), where the orientation and the arrangement of the molecule in the second monolayer are different from those in the first monolayer contacting directly with the Cu(110) surface.[30,31] In the experimental setup in Fig. 3, the electric-field vector $\boldsymbol{E}$ of the incident photon was parallel to the $[1\bar{1}0]$ substrate direction. Thus, the change in the valence electronic structure upon annealing can be explained by the symmetry selection rules (i.e., change in the lateral film structure) as will be discussed later. This result indicates that the highly ordered pentacene monolayer could also be realized in the present sample of film (ii). When the film thickness exceeds 10 nm, on the other hand, we obtained the UPS spectrum of the well-oriented pentacene multilayer of upright-standing molecular orientation (not shown). The characteristics of the UPS spectrum of the well-oriented pentacene multilayer, where the molecules orient with their plane nearly perpendicular to the substrate surface, are described elsewhere.[37] Although the valence electronic structure strongly depends on the molecular order along the substrate surface, we note that the effect of the difference of the molecular order on the interfacial dipole layer between the as-deposited [film (i)] and highly ordered film [film (ii)] is negligibly small (0.05 eV), even if it exists. The possible origin of the presently observed interface dipole layer will be discussed later.

B. Formation of the interface states

In order to discuss the valence electronic structure at the pentacene/Cu(110) interface in detail, we performed various ARUPS measurements for the highly ordered pentacene/Cu(110) system, which is prepared by the same method as that for film (ii) in Fig. 3. The ϕ dependences of the ARUPS spectra with a step of 3° for (a) the clean Cu(110) substrate and (b) the pentacene monolayer on the Cu(110) substrate are shown in Fig. 4. The abscissa is E_b relative to the substrate E_F, and the spectra are normalized to the incident photon flux. The spectra were measured at α=60°, θ=58°, and $h\nu$=20 eV. As a reference, in Fig. 4(b), we also show the UPS spectrum of the gas-phase pentacene,[38,39] which is shifted to align the lowest-E_b peak to that of the pentacene monolayer on Cu(110) at ϕ=0°. For the Cu(110) substrate, the peak S due to the direct transition from the *s*, *p* band appears at 1.9 eV when ϕ=0°, and gradually shifts toward the low-E_b side until ϕ reaches 30°. Upon formation of the pentacene monolayer on the substrate, the intensity of this substrate peak S decreases, and the pentacene-derived peaks A–C appear along with an increase of intensity at E_F.

It is interesting to note that the pentacene-derived peaks A–C shift continuously with ϕ, which may be the reflection of the two-dimensional energy-band dispersion at the surface. However, in the case of thin films of large

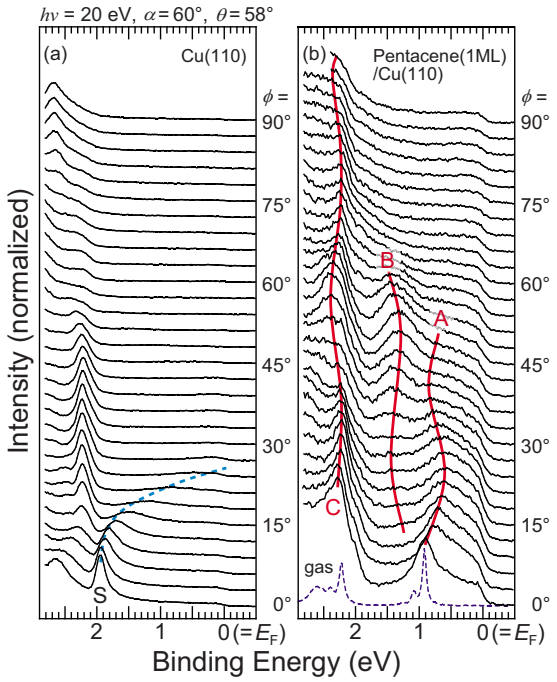

FIG. 4. (Color online) Azimuthal angle (ϕ) dependence of the ARUPS spectra for (a) the Cu(110) substrate and (b) the pentacene monolayer on Cu(110) [film (ii) in Fig. 3]. The abscissa is the binding energy relative to the Fermi level (E_F) of the substrate. The UPS spectrum of the gas-phase pentacene are shown for comparison (Refs. 38 and 39), which is shifted to align the lowest binding-energy peak to that of the pentacene monolayer on Cu(110) at ϕ =0°.

π-conjugated planar molecules with flat-lying orientation, where the intermolecular σ-σ interaction is rather weak, such a continuous peak-position change with ϕ has not been observed.[40–42] This finding of the dispersive behavior will be discussed in detail later, together with the cases with exceptionally strong lateral interaction.

Another interesting point is the relative energies among peaks A–C in Fig. 4(b). We note that the separation between A and B is about $0.6\pm0.1_2$ eV, while the E_b difference between the HOMO and HOMO-1 peaks in the gas-phase UPS spectrum is much larger (1.4 eV).[38,39] This discrepancy is in contrast to the case of the weakly physisorbed pentacene monolayer on highly oriented pyrolytic graphite with a flat-lying orientation, where the relative energies of the UPS peaks agree well with those in the gas phase, reflecting the persistence of molecular characteristics in the film.[32] Thus, we can consider that the peaks A and B are formed by the strong molecule-substrate interaction.

For further discussion of the origin of peaks A–C it is helpful to examine the symmetry selection rules for the ARUPS spectra, since they give information on the geometrical arrangements and electronic structures of adsorbates. We applied such rules to the observed ϕ dependence of peaks A–C in Fig. 4(b).

For such consideration, we use the point group of the molecule. The symmetry of the free pentacene molecule is D_{2h}. Upon flat-lying adsorption on the Cu(110) surface with-

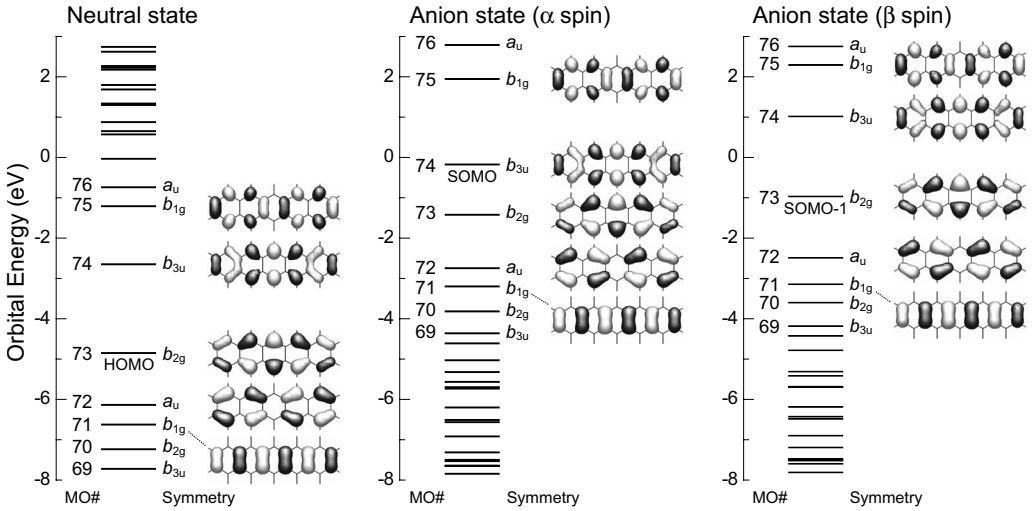

FIG. 5. The orbital energies and the corresponding symmetries of molecular orbitals of a pentacene molecule in neutral and anion states obtained from density-functional theory calculation. For the anion, we assumed that an electron with α spin occupies the original LUMO of the neutral molecule (SOMO).

out considering the distortion of the molecular plane, the symmetry is reduced to C_{2v} due to the existence of the substrate, which eliminates the molecular plane as a symmetry element. The selection rules were examined based on the MO calculations for a pentacene molecule by density-functional theory performed with the GAUSSIAN03 package using a 6-31G(d,p) basis set. Electron correlation was taken into account using Becke's three-parameter exchange with Lee, Young, and Parr correlation function. In Fig. 5 and Table I, we summarize the obtained orbital patterns and the representations in the D_{2h} and C_{2v} point groups in the neutral and anion states. For the anion, we assumed that an electron with α spin occupies the original LUMO of the neutral molecule (i.e., singly occupied molecular orbital: SOMO). In the present experimental setup, the electric vector of the light $\boldsymbol{E}$ can be regarded as almost polarized along the surface normal. To detect photoelectrons in the incident plane of light, the final state should be symmetric with respect to the incident plane. This requires that the occupied state, from which the electron is emitted, be symmetric with respect to this plane. For example, the HOMO of the neutral pentacene should show weak emission for the $[1\bar{1}0]$ substrate direction at $\phi=0°$ and strong emission for the $[001]$ substrate direction at $\phi=90°$ (denoted in Table I by $\times$ and $\bigcirc$, respectively). However, as seen in Fig. 4(b), the lowest-E_b peak (A) of the pentacene monolayer on Cu(110) shows strong emission for the $[1\bar{1}0]$ substrate direction at $\phi=0°$ and no emission for the $[001]$ substrate direction at $\phi=90°$, which do not agree with the photoemission behavior expected from the symmetry selection rules.

Since the simple consideration mentioned above does not work, we rather judged the representations for the levels A–C from their observed behaviors in the spectra in Fig. 4(b) based on the selection rules listed in Table I. From such examination, the peaks A, B, and C can be assigned to b_1, b_1 (or a_2), and a_1 representations in the C_{2v} symmetry, respectively, as summarized in Table II. As the possible origins of the discrepancy from the orbital patterns for a free molecule, we propose that peaks A and B may originate from (i) the energy level splitting of the original HOMO level due to the hybridization with the wave function of the substrate, (ii) different molecular levels which are each for itself modified by admixtures of metal states, or (iii) the modification of the surface electronic structure of the Cu(110) substrate due to the adsorption of the molecule. These phenomena can modify the orbital symmetry. Peak C can also be assigned to the resultant interface states. Further considerations on the origin of the interface state at the pentacene/Cu(110) inter-

TABLE I. Summary of the orbital symmetry for gas-phase (D_{2h}) and flat-lying-oriented (C_{2v}) pentacene. The allowed and forbidden transitions for the emission in the incident plane of photon are denoted by $\bigcirc$ and $\times$, respectively. Orbital numbers correspond to those in Fig. 5.

Orbital number	Symmetry		$[1\bar{1}0]$ ($\phi=0°$)	$[001]$ ($\phi=90°$)
	D_{2h}	C_{2v}		
74	b_{3u}	a_1	$\bigcirc$	$\bigcirc$
73	b_{2g}	b_2	$\times$	$\bigcirc$
72	a_u	a_2	$\times$	$\times$
71	b_{1g}	b_1	$\bigcirc$	$\times$

TABLE II. Assignments of the experimentally observed peaks A–C in C_{2v} symmetry estimated from the examination of the symmetry selection rule (see Table I).

Peak in Fig. 4	$[1\bar{1}0]$ ($\phi=0°$)	$[001]$ ($\phi=90°$)	Assignment (in C_{2v} symmetry)
A	$\bigcirc$	$\times$	b_1
B	Hidden	$\times$	b_1 or a_2
C	$\bigcirc$	$\bigcirc$	a_1

face are now in progress by comparing with theoretical calculations.

Next we discuss the steplike feature in the ϕ dependence of the UPS line shape near E_F of the pentacene/Cu(110) system, which cannot be explained by the background of the Fermi edge of the Cu(110) substrate, which weakly appears in the spectra of clean Cu(110) substrate.

It was reported for pentacene/Cu(110) that the C 1*s* and Cu 3*p* XPS spectra showed different line shapes between the monolayer and the multilayer coverage.[15] For the monolayer film, the core-level photoemission line shape could be explained assuming electron transfer from the substrate to the pentacene molecule.[15] On the other hand, the strong electronic coupling of the MOs with the substrate was suggested from NEXAFS study. The π^*-resonance line shape due to the transitions from the various C 1*s* levels into unoccupied states for the pentacene *multilayer* on Cu(110) (Refs. 30 and 31) corresponds well with that for the pentacene *monolayer* on Au(111).[43] However, the π^*-resonance line shape for pentacene monolayer on Cu(110) is clearly different from these cases.[30,31] For the origin of the π^*-resonance line shape for pentacene monolayer on Cu(110), Lukas *et al.*[30,31] suggest a pronounced electronic distortion, or rehybridization, of the MOs upon adsorption on the Cu(110) surface.

Combining the previous XPS and NEXAFS results, we consider that one possible origin of the observed steplike feature near E_F is the (former) LUMO-derived state, which is occupied by an electron from the substrate due to the strong molecule-substrate interaction and the hybridization with the wave function of the substrate. Similar scenario has been reported by using the interfaces of perylene-3,4,9,10-tetracarboxylic acid dianhydride (PTCDA) on Ag(111) and Ag(110),[7,19,20] and of benzene on Ni(100) and Cu(110).[44] Second possible origin of the steplike feature near E_F is the modification of the photoionization cross section for the substrate E_F due to the change in the symmetry of the substrate surface upon adsorption. Third is the formation of the IDIS[21] or the metal-induced gap state.[45] Such effect was suggested at the pentacene/Au(001) interface by Lee *et al.*, with the theoretical calculation as a function of the molecule-substrate distance.[46]

C. Intermolecular energy-band dispersion via the substrate

As mentioned above, the pentacene-derived peaks A–C in Fig. 4(b) show continuous position change with ϕ. This may be ascribed to the two-dimensional intermolecular energy-band dispersion. However, it is difficult to precisely discuss the observed shift due to the possible coexistence of the $p(6.5\times2)$ and the $c(13\times2)$ [or the $p(6\times2)$ and the $c(12\times2)$] overlayers reported in Refs. 29–31. As seen in Fig. 2, the Brillouin zones for the $p(6.5\times2)$ and the $c(13\times2)$ [or the $p(6\times2)$ and the $c(12\times2)$] overlayers are the same size in the $[1\bar{1}0]$ substrate direction. Thus, we can fairly discuss the periodicity of the energy-band dispersion along the $[1\bar{1}0]$ substrate direction.

In order to discuss the observed continuous peak-position change in Fig. 4(b) further, we examined the θ dependence of the ARUPS spectra at $\phi=0°$, which corresponds to the

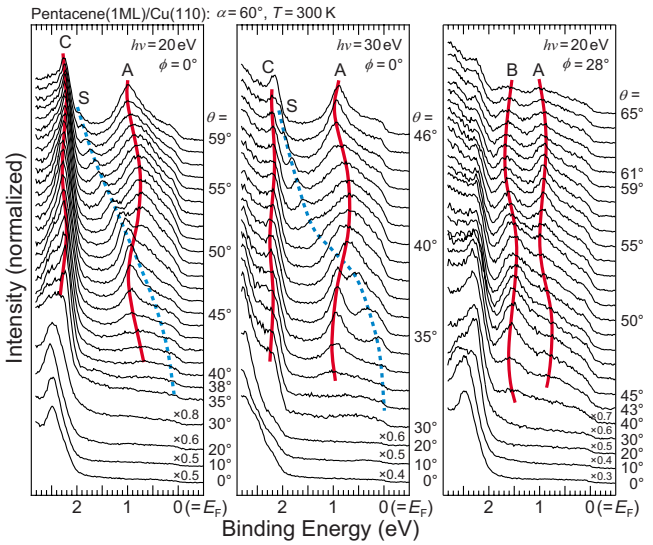

FIG. 6. (Color online) Takeoff angle (θ) dependence of the ARUPS spectra for the pentacene monolayer on Cu(110) measured at $\phi=0°$, which corresponds to the $[1\bar{1}0]$ substrate direction, and $\phi=28°$, which shows peaks A and B in Fig. 4 simultaneously, with $h\nu$ of 20 and 30 eV. The abscissa is the binding energy relative to the Fermi level (E_F) of the substrate.

$[1\bar{1}0]$ substrate direction, and $\phi=28°$, which shows peaks A and B in Fig. 4 simultaneously. In our experimental setup, we could not observe peaks A–C from the θ dependences of the ARUPS spectra along the [001] substrate direction ($\phi=90°$) except for the Shockley-type surface state localized around the $\bar{Y}$ point, probably due to the symmetry selection rule and the existence of the substrate background. The results at $\phi=0°$ and 28° are shown in Fig. 6. The spectra were measured at $\alpha=60°$ with $h\nu=20$ and 30 eV, and the intensities are normalized to the incident photon flux. At $\phi=0°$, for both $h\nu=20$ and 30 eV, the direct transition peak S from the *s*,*p* band of the substrate shows a large dispersion with θ between $E_b=0$ and 2 eV as indicated by dashed (blue) curve. This agrees well with the previous reports.[34–36] For the pentacene-derived peak A, the periodic shift of the peak with θ is also clearly seen. At $\phi=0°$, $\theta=40°$, and $h\nu=20$ eV, the value of E_b for peak A is about 0.7 eV. With increasing θ, it shifts to the high-E_b side, and turns back at $\theta=45°$. We see a similar turning of peak A also at $\theta=50°$ and 58°. The total width of the shift is about 0.25 eV. Furthermore, peak C also shows a somewhat smaller periodic shift with θ, in which the total width of the shift is about 0.05 eV. These periodic shifts can also be seen for $h\nu=30$ eV. On the other hand, at $\phi=28°$, one can see the periodic shifts for both peaks A and B, and the direction of the periodic shift in peak B is opposite to that in peak A.

We will analyze these data in more detail. The photoemission process can be expressed as sequential steps of optical transition, transport to the surface, and the escape across the surface.[47] At the optical transition, both the energy and momentum are conserved. In the case of examining the θ dependence of the ARUPS spectra, we can also use the conservation of the momentum parallel to the sample surface, due

to the lack of potential step along the surface. From these relations, the lateral wave vector of photoelectron in the solid ($\boldsymbol{k}_{\parallel}$) is expressed as

$$\boldsymbol{k}_{\parallel} = \frac{\sqrt{2m_e^* E_k}}{\hbar} \sin\theta, \tag{1}$$

where m_e^* is the effective mass of the photoelectron and E_k is the kinetic energy relative to the vacuum level.[47]

To confirm the validity of the preceding discussion, it is also necessary to examine the experimental resolution of the wave number ($\Delta\boldsymbol{k}_{\parallel}$) since the lattice constant is large in the present sample. This can be obtained by differentiating Eq. (1) as

$$\Delta\boldsymbol{k}_{\parallel} = \frac{\sqrt{m_e^*}}{\hbar}\left(\frac{\Delta E_k}{\sqrt{2E_k}} \sin\theta + \sqrt{2E_k}\cos\theta\Delta\theta\right). \tag{2}$$

In the present experiments, the values of $\Delta\theta$ and ΔE_k are 2° and 0.1 eV, respectively. Consequently, $\Delta\boldsymbol{k}_{\parallel}$ is largest at the Γ point of the topmost band and is estimated to be less than 0.9 nm^{-1}, which is equivalent to about 23% of the width of the Brillouin zone. Thus, the uncertainty in the wave vector is not negligible, but still sufficiently small to allow the discussion made below.

Figure 7 shows the experimentally derived band structure at ϕ=0° (the [1$\bar{1}$0] substrate direction) and ϕ=28° obtained by using Fig. 6 and Eq. (1). The abscissa is the lateral wave vector $\boldsymbol{k}_{\parallel}$, and the ordinate is E_b relative to the substrate E_F. In order to map out the energy-band dispersion, we took the second derivative of the ARUPS spectra $[-d^2I(E_b)/dE_b^2]$ at $h\nu$=20 eV after smoothing to specify the energies of the spectral features. Open and filled circles indicate the peak position of peaks A–C in the ARUPS spectra measured at $h\nu$=20 and 30 eV, respectively. The labels Γ_A and Γ_B in Fig. 7(a) indicate the expected Γ points from the previous structural analyses of the $p(6.5\times2)$ structure[30,31] and the $p(6\times2)$ structure[29], respectively. One can see that the $E(\boldsymbol{k}_{\parallel})$ curve of peak A measured at $h\nu$=20 eV corresponds well with that measured at $h\nu$=30 eV, and that the $E(k_{\parallel})$ curve of peak C has turning points at the same $\boldsymbol{k}_{\parallel}$ positions as that for peak A. From the present experiments, we found that the experimentally observed Γ point (Γ_{exp}) exists at $\boldsymbol{k}_{\parallel}$ =15.7±0.9 nm^{-1}, which is the center of the fifth Brillouin zone, and the Γ_{exp} fairly well agrees with the expected Γ points of Γ_A and Γ_B. Furthermore, from the band structure at ϕ=28° shown in Fig. 7(b), we confirmed that the turning points of the $E(\boldsymbol{k}_{\parallel})$ curve for peak B appear at the same $\boldsymbol{k}_{\parallel}$ as that for peak A, and that the phase of the curve for peak B is opposite to that of peak A.

From the $E(\boldsymbol{k}_{\parallel})$ curves of peaks A and C, we can estimate the lattice constant (λ) along the [1$\bar{1}$0] substrate direction using the relation $\lambda=2\pi/K$, where K is the size of the Brillouin zone, under the assumption of the tight-binding model. The value of λ obtained from the data in Fig. 7 is about 1.6 nm, which agrees well with the lattice constant estimated from the previous HAS and LEED measurements.[29–31] These findings support our assignments that the periodic shift of peaks A–C are due to the in-plane intermolecular energy-band dispersion in the pentacene monolayer on Cu(110). By assuming peak A in Fig. 7 to be a free-electron-like dispersion parabola, the effective mass of the photohole (m_h^*) is obtained to be $0.24m_0$ at 300 K. On the other hand, there is a flatband just below the substrate E_F. It can be a (former) LUMO-derived state of the molecule, which is partially occupied by an electron from the substrate, or some other gap state strongly localized at the interface as discussed above.

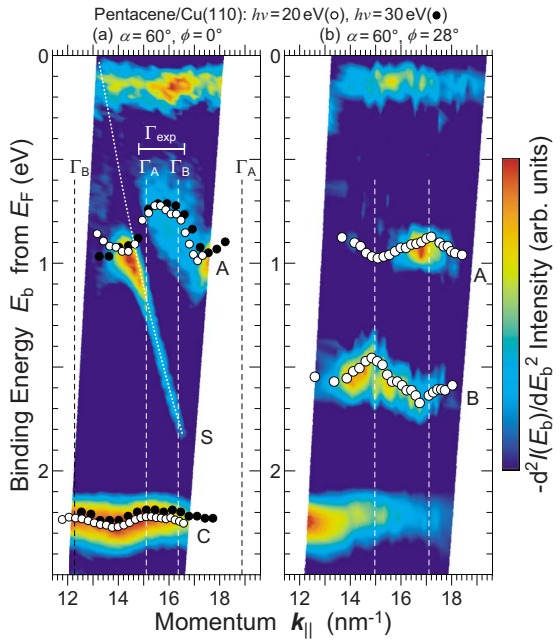

FIG. 7. (Color online) In-plane intermolecular energy-band dispersion in the pentacene monolayer on Cu(110) at ϕ=0° (the [1$\bar{1}$0] substrate direction) and ϕ=28°. The abscissa is the parallel component of the wave vector ($k_{\parallel}$), and the ordinate is the binding energy (E_b) relative to the Fermi level (E_F) of the substrate. In order to map out the energy-band dispersion, we took the second derivative of the ARUPS spectra $[-d^2I(E_b)/dE_b^2]$ at $h\nu$=20 eV after smoothing to specify the energies of the spectral features. The labels A, B, C, and S correspond to those in Fig. 6. Open and filled circles indicate the position of the pentacene-derived peaks in the raw ARUPS spectra measured at $h\nu$=20 and 30 eV, respectively.

From the structural analyses on the pentacene/Cu(110), the pentacene monolayer forms the coexistent layer with the $p(6.5\times2)$ and the $c(13\times2)$ [or the $p(6\times2)$ and the $c(12\times2)$] phases.[29–31] In the [1$\bar{1}$0] substrate direction, the $p(6.5\times2)$ and the $c(13\times2)$ [or the $p(6\times2)$ and the $c(12\times2)$] overlayers have their Γ points at the same $\boldsymbol{k}$ position. Thus, we note that (i) the turning point of the $E(\boldsymbol{k}_{\parallel})$ curve along the [1$\bar{1}$0] substrate direction fairly reflects the Γ point of the film, and that (ii) the bandwidth and the estimated m_h^* are the averaged values over the $p(6.5\times2)$ and the $c(13\times2)$ [or the $p(6\times2)$ and the $c(12\times2)$] phases.

The observation of in-plane intermolecular energy-band dispersion in flat-lying π-conjugated organic thin films has been reported for the benzene/metal systems.[48–50] In these systems, such a dispersion was observed for the σ-derived MOs, and has been explained by the compressed film structure with the small intermolecular distance forced by the un-

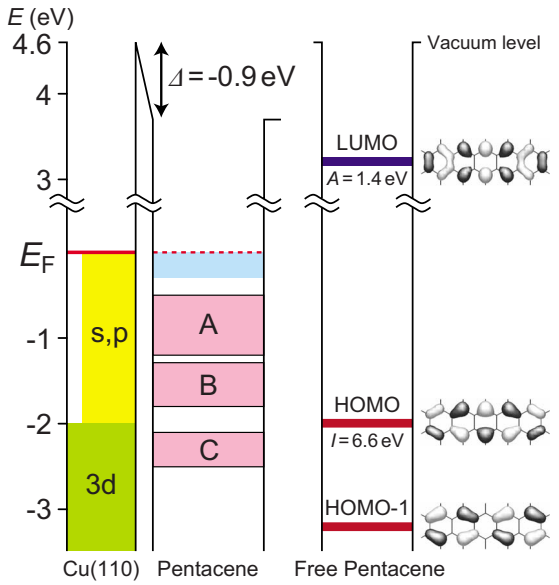

FIG. 8. (Color online) Energy level diagram for the pentacene/Cu(110) interface. Energy levels for free pentacene molecules are shown for comparison. For free pentacene, the ionization energy (I) was obtained from Refs. 38 and 39, and the electron affinity (A) was estimated from Ref. 6.

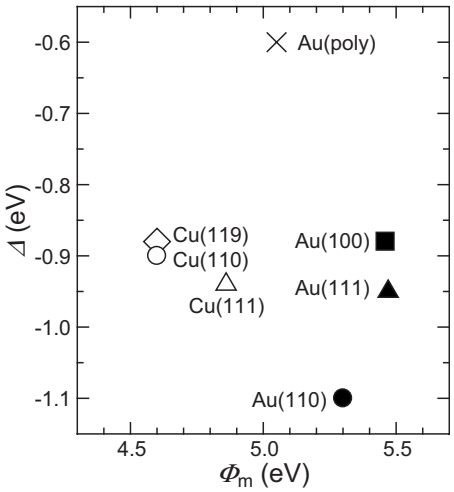

FIG. 9. Plots of the interface dipole (Δ) against the work function of the metal (Φ_m) for various pentacene/metal interfaces.

derlying substrate. Such a compressed structure induces strong intermolecular σ-σ interaction. In the present system of pentacene/Cu(110), however, the film structure is not compressed as judged from the lattice constant and the van der Waals radii compared with benzene/metal. On the other hand, Temirov *et al.* reported the in-plane intermolecular energy-band dispersion for the unoccupied state in a PTCDA monolayer on Ag(111) with an effective mass of electron of $0.47m_0$ from the high-resolution STM with STS study.[20] The observed dispersion in Ref. 20 is far larger than expected for the PTCDA monolayer alone,[51] and they suggest that the dispersion might be related to the surface state since the effective mass is similar to that of the Ag(111) surface. However, in the present pentacene/Cu(110) case, there is no known surface state along the $[1\bar{1}0]$ substrate direction on the Cu(110) surface within the observed energy window.[34–36]

Although we cannot give a definite origin of this dispersion at present, we can deduce that the intermolecular interaction via direct contact is considerably weak, and the observed dispersion may originate from the intermolecular interaction via the substrate due to the significant hybridization between the MOs and the substrate. For further consideration about this issue, a joint experimental and theoretical study is now in progress.

D. Energy level alignment at pentacene/Cu(110) interface

Finally, we discuss the possible origin and the characteristics of the interface dipole for the pentacene/Cu(110) interface. We summarize the energy diagram for the pentacene/Cu(110) interface in Fig. 8. From the UPS spectra in Fig. 3, the work function of the clean Cu(110) surface is 4.6 eV and its change (Δ) by the adsorption of pentacene is about −0.9 eV (negative Δ), which does not so much depend on the lateral film structure and the energy-band formation. This value corresponds to the magnitude of the dipole layer, with the molecular side positively charged.

On the other hand, judging from the previous XPS experiments,[15] electron transfer from the Cu(110) substrate to the pentacene layer can be expected. If this is the main cause of the dipole layer, a *positive* Δ should be observed. Thus, the experimental observation of the negative Δ indicates that the presently observed interface dipole cannot be explained by the simple charge-transfer scenario only. Moreover, a similar negative value of Δ has been observed for various pentacene/metal interfaces as summarized in Fig. 9.[3,6,14,15]

This apparent discrepancy indicates that other important origins of the interface dipole operate besides charge transfer for the present case of the pentacene/Cu(110) interface. As candidates of such mechanisms, we can list, for example, the image effect and the push-back effect. The image effect is discussed as a possible explanation for the Xe/metal system.[52] When an electron in the adsorbate comes close to the metal surface, it induces an image charge in the metal, and the electron and the image attract each other, leaving the vacuum side positive. In the push-back mechanism, the electron cloud of metal spilled out into the vacuum is pushed back by the adsorption of a molecule due to the repulsion with the electrons in the adsorbate. In this case, the net change between the clean and the adsorbed surface corresponds to the formation of an additional dipole layer, with the vacuum side positive.[1] Thus, both of these factors lower the work function.

It was reported for the interface of weakly physisorbed benzene/Al(111) that the observed negative Δ of −0.2 eV upon the monolayer adsorption can be explained by the Pauli repulsion (i.e., push-back effect) even though the molecule is relatively far from the surface.[25] In the present case of the pentacene/Cu(110) interface with strong molecule-substrate interaction, the factors of the image effect and the push-back effect may have overwhelmed the effect of electron transfer,

which raises the work function. In particular, the key parameter in the push-back effect is the molecule-substrate distance as discussed by Morikawa *et al.*[26] As seen in Fig. 9, the magnitude of Δ for the pentacene thin films prepared on the Au polycrystalline substrate is smaller than that for films on the Au single crystal substrate. In the case of the polycrystalline substrate with possibly rough surface, the molecular orientation and the molecule-substrate distance may vary depending on the substrate surface, producing smaller Δ than in the case of the single crystal substrate. For further discussion on the origin of Δ at organic/metal interfaces, we need more detailed information on the interfacial electronic structure and molecule-substrate distance, which can be obtained, e.g., from the x-ray standing wave experiments.[53–55]

IV. SUMMARY

In this work, we performed precise angle-resolved photoemission study on the electronic structure of the highly ordered pentacene/Cu(110) interface. We have observed the distinctive electronic structure at the interface with the following findings: (i) formation of the interface states with possible modification of the orbital symmetry and the energy position, and (ii) two-dimensional intermolecular energy-band dispersion of these interface states with the bandwidth for the upper branch being 0.25 eV. From the observed energy-band dispersion, the effective mass of the photohole is estimated to be $0.24m_0$ at 300 K. These interface states can be deduced to originate from the hybridization between the MOs and the wave function of the substrate, which may also lead to the observed energy-band dispersion by the intermolecular interaction through the substrate. From the secondary-electron cutoff, we also obtained the magnitude and the direction of the interface dipole to be about −0.9 eV, which cannot be explained by the simple charge transfer scenario. We proposed the image effect and the push-back effect as possible and important origins for the presently observed interface dipole as well as the charge transfer.

V. CONCLUDING REMARKS

Finally, we will examine the implication of the presently observed results for the study of organic/metal interfaces, which are important not only in themselves but also for the rapidly growing organic and molecular electronics. The present study clearly showed that the interaction of the first molecular layer with the metal can be fairly strong and complex, including various factors. Thus, the systematic accumulation of the reliable and precise data for various well-defined interfaces as obtained here will be necessary to clarify the general picture of organic/metal interfaces.

Also, we note that the factors introduced in real interfaces should be also taken into account to discuss the interfaces in relation to various devices. For example, the reported fair agreement between the simple charge-transfer scenario of the interfacial dipole layer in terms of the concept of IDIS and CNL is based on the comparison with the experiments in ultrahigh vacuum, but using polycrystalline evaporated metal substrates with possibly rough surfaces. Also, the evaporated organic films are mostly amorphous or polycrystalline. Such interfaces may be different from those for atomically flat metal surfaces as studied here in various ways, and there may be some possibility that such nonideal factors may cancel some effects for ideal interfaces, leading to the apparent validity of the simple charge-transfer scenario. For the comparison with the real devices, we should further take account of additional factors such as the effect of atmospheric gases and various contaminants, or the interdiffusion of the species at the interface.

Thus, the relation of the studies of well-defined systems as carried out here with the real device performance may not be so straightforward, but the full clarification of such well-defined systems is still important, as pure science and also as the basis of the studies oriented to real devices. Parallel studies of well-defined systems and realistic factors altogether will lead to fruitful perspective both in pure science and the real applications.

ACKNOWLEDGMENTS

The authors thank the UVSOR staff for their support in various ways, and are grateful to K. Lee (National Renewable Energy Laboratory, USA) and Y. Morikawa (Osaka University, Japan) for fruitful discussion with their theoretical calculation. H.Y. acknowledges support from the Japan Society for the Promotion of Science (JSPS). The present work was partly supported by the Grant-in-Aid for Creative Scientific Research (Grant No. 14GS0213) from JSPS and the 21st Century Center-of-Excellence Program [Establishment of COE on Material Science: Elucidation and Creation of Molecular Functions (Nagoya University) and Frontiers of Super-Functionality Organic Devices (Chiba University)] from the Ministry of Education, Culture, Sports, Science, and Technology of Japan.

[1] H. Ishii, K. Sugiyama, E. Ito, and K. Seki, Adv. Mater. (Weinheim, Ger.) **11**, 605 (1999).

[2] *Conjugated Polymers and Molecular Interfaces: Science and Technology for Photonic and Optoelectronic Applications*, edited by W. R. Salaneck, K. Seki, A. Kahn, and J.-J. Pireaux (Dekker, New York, 2002).

[3] P. G. Schroeder, C. B. France, J. B. Park, and B. A. Parkinson, J. Appl. Phys. **91**, 3010 (2002).

[4] T. Munakata, T. Sugiyama, T. Masuda, M. Aida, and N. Ueno, Appl. Phys. Lett. **85**, 3584 (2004).

[5] T. Schwieger, H. Peisert, and M. Knupfer, Chem. Phys. Lett. **384**, 197 (2004).

[6] F. Amy, C. Chan, and A. Kahn, Org. Electron. **6**, 85 (2005).

[7] Y. Zou, L. Kilian, A. Schöll, Th. Schmidt, R. Fink, and E. Umbach, Surf. Sci. **600**, 1240 (2006).

[8] N. Koch, S. Duhm, J. P. Rabe, A. Vollmer, and R. L. Johnson,

Phys. Rev. Lett. **95**, 237601 (2005).
[9] L. Lindell, M. P. de Jong, W. Osikowicz, R. Lazzaroni, M. Berggren, W. R. Salaneck, and X. Crispin, J. Chem. Phys. **122**, 084712 (2005).
[10] I. H. Campbell J. D. Kress, R. L. Martin, D. L. Smith, N. N. Barashkov, and J. P. Ferraris, Appl. Phys. Lett. **71**, 3528 (1997).
[11] M. Fujihira and C. Ganzorig, in *Conjugated Polymers and Molecular Interfaces: Science and Technology for Photonic and Optoelectronic Applications* (Ref. 2), Chap. 26.
[12] S. Kera, Y. Yabuuchi, H. Yamane, H. Setoyama, K. K. Okudaira, A. Kahn, and N. Ueno, Phys. Rev. B **70**, 085304 (2004).
[13] H. Fukagawa, S. Kera, T. Kataoka, S. Hosoumi, Y. Watanabe, K. Kudo, and N. Ueno, Adv. Mater. (Weinheim, Ger.) **19**, 665 (2007).
[14] C. Baldacchini, C. Mariani, and M. G. Betti, J. Chem. Phys. **124**, 154702 (2006).
[15] O. McDonald, A. A. Cafolla, D. Carty, G. Sheerin, and G. Hughes, Surf. Sci. **600**, 1909 (2006).
[16] M. Takada and H. Tada, Ultramicroscopy **105**, 22 (2005).
[17] M. Takada and H. Tada, Jpn. J. Appl. Phys., Part 1 **44**, 5332 (2005).
[18] J. Repp, G. Meyer, S. Paavilainen, F. E. Olsson, and M. Persson, Science **312**, 1196 (2006).
[19] A. Kraft, R. Temirov, S. K. M. Henze, S. Soubatch, M. Rohlfing, and F. S. Tautz, Phys. Rev. B **74**, 041402(R) (2006).
[20] R. Temirov, S. Soubatch, A. Luican, and F. S. Tautz, Nature (London) **444**, 350 (2006).
[21] C. Tejedor, F. Flores, and E. Louis, J. Phys. C **10**, 2163 (1977).
[22] H. Vázquez, R. Oszwaldowski, P. Pou, J. Ortega, R. Pérez, F. Flores, and A. Kahn, Europhys. Lett. **65**, 802 (2004).
[23] H. Vázquez, F. Flores, R. Oszwaldowski, J. Ortega, R. Pérez, and A. Kahn, Appl. Surf. Sci. **234**, 107 (2004).
[24] H. Vázquez, W. Gao, F. Flores, and A. Kahn, Phys. Rev. B **71**, 041306(R) (2005).
[25] R. Duschek, F. Mittendorfer, R. I. R. Blyth, F. P. Netzer, J. Hafner, and M. G. Ramsey, Chem. Phys. Lett. **318**, 43 (2000).
[26] Y. Morikawa, H. Ishii, and K. Seki, Phys. Rev. B **69**, 041403(R) (2004).
[27] P. S. Bagus, K. Hermann, and Ch. Wöll, J. Chem. Phys. **123**, 184109 (2005).
[28] S. Lukas, G. Witte, and Ch. Wöll, Phys. Rev. Lett. **88**, 028301 (2001).
[29] Q. Chen, A. J. McDowall, and N. V. Richardson, Langmuir **19**, 10164 (2003).
[30] S. Lukas, S. Söhnchen, G. Witte, and Ch. Wöll, ChemPhysChem **5**, 266 (2004).
[31] S. Söhnchen, S. Lukas, and G. Witte, J. Chem. Phys. **121**, 525 (2004).
[32] H. Yamane, S. Nagamatsu, H. Fukagawa, S. Kera, R. Friedlein, K. K. Okudaira, and N. Ueno, Phys. Rev. B **72**, 153412 (2005).
[33] K. Seki, H. Nakagawa, K. Fukui, E. Ishiguro, R. Kato, T. Mori, K. Sakai, and M. Watanabe, Nucl. Instrum. Methods Phys. Res. A **246**, 264 (1986).
[34] K. Berge, A. Gerlach, G. Meister, A. Goldmann, and J. Braun, Surf. Sci. **498**, 1 (2002).
[35] K. Berge and A. Goldmann, Surf. Sci. **540**, 97 (2003).
[36] P. Cortona and C. Sapet, Int. J. Quantum Chem. **99**, 713 (2004).
[37] H. Fukagawa, H. Yamane, T. Kataoka, S. Kera, M. Nakamura, K. Kudo, and N. Ueno, Phys. Rev. B **73**, 245310 (2006).
[38] M. S. Deleuze, A. B. Trofimov, and L. S. Cederbaum, J. Chem. Phys. **115**, 5859 (2001).
[39] V. Coropceanu, M. Malagoli, D. A. da Silva Filho, N. E. Gruhn, T. G. Bill, and J. L. Brédas, Phys. Rev. Lett. **89**, 275503 (2002).
[40] N. Ueno, A. Kitamura, K. K. Okudaira, T. Miyamae, Y. Harada, S. Hasegawa, H. Ishii, H. Inokuchi, T. Fujikawa, T. Miyazaki, and K. Seki, J. Chem. Phys. **107**, 2079 (1997).
[41] K. K. Okudaira, S. Hasegawa, H. Ishii, K. Seki, Y. Harada, and N. Ueno, J. Appl. Phys. **85**, 6453 (1999).
[42] S. Kera, S. Tanaka, H. Yamane, D. Yoshimura, K. K. Okudaira, K. Seki, and N. Ueno, Chem. Phys. **325**, 113 (2006).
[43] G. Beernink, T. Strunskus, G. Witte, and Ch. Wöll, Appl. Phys. Lett. **85**, 398 (2004).
[44] A. Nilsson, N. Wassdahl, M. Weinelt, O. Karis, T. Wiell, P. Bennich, J. Hasselström, A. Föhlisch, J. Stöhr, and M. Samant, Appl. Phys. A: Mater. Sci. Process. **65**, 147 (1997).
[45] J. Tersoff, Phys. Rev. Lett. **52**, 465 (1984).
[46] K. Lee, J. Yu, and Y. Morikawa, Phys. Rev. B **75**, 045402 (2007).
[47] *Angle-resolved Photoemission: Theory and Current Applications*, edited by S. D. Kevan (Elsevier, Amsterdam, 1992).
[48] F. P. Netzer, Vacuum **41**, 49 (1990).
[49] M. G. Ramsey, D. Steinmüller, F. P. Netzer, T. Schedel, and A. Santaniello, Surf. Sci. **251/252**, 979 (1991).
[50] H. H. Graen, M. Neuber, M. Neumann, G. Odörfer, and H.-J. Freund, Europhys. Lett. **12**, 173 (1990).
[51] H. Yamane, S. Kera, K. K. Okudaira, D. Yoshimura, K. Seki, and N. Ueno, Phys. Rev. B **68**, 033102 (2003).
[52] K. Wandelt and J. E. Hulse, J. Chem. Phys. **80**, 1340 (1984).
[53] A. Hauschild, K. Karki, B. C. C. Cowie, M. Rohlfing, F. S. Tautz, and M. Sokolowski, Phys. Rev. Lett. **94**, 036106 (2005).
[54] A. Gerlach, S. Sellner, F. Schreiber, N. Koch, and J. Zegenhagen, Phys. Rev. B **75**, 045401 (2007).
[55] S. K. M. Henze, O. Bauer, T.-L. Lee, M. Sokolowski, and F. S. Tautz, Surf. Sci. **601**, 1566 (2007).